

# Verification of the Concept of Seismoionospheric Coupling under Quiet Heliogeomagnetic Conditions, Using the Wenchuan (China) Earthquake of May 12, 2008, as an Example

S. A. Pulinets<sup>a, b</sup>, V. G. Bondur<sup>a</sup>, M. N. Tsidilina<sup>a</sup>, and M. V. Gaponova<sup>a</sup>

<sup>a</sup> “Aerocosmos” Scientific Center for Aerospace Monitoring, Moscow, Russia

<sup>b</sup> Fiodorov Institute of Applied Geophysics, Roshydromet, Moscow, Russia

e-mail: pulse1549@gmail.com

Received July 15, 2009; in final form, August 25, 2009

**Abstract**—The variability of the ionosphere during April–May, 2008, has been analyzed in detail in order to reveal anomalous variations related to seismic activity, initiated by the strongest Wenchuan earthquake ( $M = 7.9$ ) in the Sichuan province on May 12, 2008. Information about the total electron content (TEC) from the network of GPS receivers in the earthquake region, the global IONEX TEC maps, and the reconstructed vertical profiles of electron density according to the data of GPS receivers were used as a data source. The spatial and time localization of the observed anomalies, their morphological features, and the absence of geomagnetic disturbances during the observation period undoubtedly demonstrate that the observed variations were caused by seismic activity.

**DOI:** 10.1134/S0016793210020118

## 1. INTRODUCTION

The fact that specific variations in the ionosphere are related to seismic activity and appear over the earthquake preparation region several days before a seismic shock has been proved by numerous publications [Pulinets et al., 1994; Chuo et al., 2001; Zakharenkova et al., 2006], statistical studies [Pulinets et al., 2002; Liu et al., 2004, 2006], and the physical mechanism [Pulinets and Boyarchuk, 2004; Pulinets 2009a]; however, this fact is still discussed in the literature including the recent publications [Afraimovich and Astafyeva, 2008]. A high variability of the ionosphere and the effects related to solar activity are still the main arguments against this fact. Therefore, the periods when such activity was minimal while the ionospheric effects were significant are of great interest, which makes the arguments mentioned above not actual.

The last minimum of solar activity was characterized by extremely prolonged duration (a delay of about 2 years) and extremely low solar activity (almost completely absent sunspots and pronounced solar events). This makes it possible to verify different sources of ionospheric variability independent of solar activity. The atmospheric electric field [Pulinets et al., 1998a] and one of its generators (seismic activity [Pulinets, 1998]) are among such sources.

The 2007s–2008s, coinciding with a deep solar activity minimum, are characterized by very high glo-

bal solar activity. The destructive Wenchuan Chinese earthquake, which occurred in the Sichuan province on May 12, 2008, was one of the manifestations of this activity. The main earthquake parameters will be presented in the next section, and we now consider the morphological indications of the ionospheric precursors, the discussion of which will be the main matters at issue in this work.

## 2. MORPHOLOGICAL INDICATIONS OF EARTHQUAKE IONOSPHERIC PRECURSORS

In this section we will use the results achieved in [Pulinets et al., 1998b, 2003; Pulinets and Legen’ka, 2002, 2003; Liu et al., 2004]. The spatial and time localization of anomalous variations, observed in the ionosphere relative to the epicenter position and seismic shock time, are naturally the first and main indications. As was demonstrated using the satellite mapping of the ionosphere [Pulinets and Legen’ka 2003], anomalous variations appear over the earthquake preparation region, the dimension of which is defined by the  $R = 10^{0.43M}$  ratio ( $R$  is the radius of the earthquake preparation region, and  $M$  is the earthquake magnitude) [Dobrovolskii, 1991]. The order of magnitude of the anomaly extension in the ionosphere corresponds to the  $R$  estimate; however, the anomaly shape and location depends on latitude: at low latitudes, the equatorial anomaly electromagnetic nature

results in the origination of anomalous variations not only over the epicenter but also in the magnetically conjugate region. In addition, the longitudinal effect, related to the appearance of the zonal electric field [Pulinets, 2009b], is observed in the low-latitude ionosphere. In any case ionospheric variations over the earthquake preparation region differ from global variations in the ionosphere, which is one of the indications that make it possible to identify ionospheric precursors.

The statistical studies indicated [Pulinets, 1998; Liu et al., 2004, 2006] that ionospheric precursors appear on average 5 days before a seismic shock. In this case, ionospheric precursors are short-lived (with a duration of about 4 h) in contrast to effects of magnetic storms, when the negative phase in the ionosphere can last a day and more, but appear every day (or every other day) during several days usually at the same time of day [Pulinets et al., 2003]. Negative deviations of electron density are observed before the sunrise (3–5 h a.m.) at middle and high latitudes [Pulinets et al., 1998b] and in the afternoon (14–18 h p.m.) in the low-latitude ionosphere [Liu et al., 2004, 2006]. Positive variations are usually observed in the prenoon hours (10–12 h a.m.) [Pulinets et al., 1998b].

If the earthquake epicenter is at low latitudes, the electrodynamic effects in the equatorial anomaly, resulting in a change in the position and shape of equatorial anomaly crests [Pulinets and Legen'ka, 2002], should be taken into account. Specifically, it is indicated that equatorial anomaly crests move toward the geomagnetic equator before an earthquake, which is the main cause of negative anomalies in the post-noon hours within a crest and on its outer descending branch and can result in positive anomalies near the geomagnetic equator. If a low-latitude seismoionospheric effect is related to a change in the air conductivity in the Earth–ionosphere column, ionospheric effects (a change in the shape and intensity of the equatorial anomaly) can be observed west or east of an epicenter rather than exactly over this region [Pulinets, 2009b].

Seismoionospheric effects are observed not only at an electron density maximum in the ionosphere (although the variation amplitude is maximal in the density peak region) but also in the entire ionosphere: from the *D* region up to the magnetosphere [Pulinets and Boyarchuk, 2004]. Variations in the scale height of the electron density vertical profile in the ionosphere are one of the indicators of such changes. Negative electron density variations at a maximum of the ionospheric *F* region (and negative TEC variations) are accompanied by an increase in the scale height [Pulinets et al., 2007], which is one more distinctive feature of ionospheric precursors. A change in the scale height is usually related to a variation in the average ion mass. Specifically, an increase in the scale height can be explained by an increased percentage of light ions in

the total ion content. The appearance of light ions in the ionospheric *F* region before strong earthquakes was repeatedly registered in different space experiments [Bošková et al., 1993].

Thus the following morphological indications of ionospheric precursors will be studied in the present work:

- (1) The localization in space and time, including the lead time of the precursor appearance before a seismic shock.
- (2) The dependence of precursors on the local time and their regular appearance during several days before an earthquake.
- (3) The effects in the equatorial anomaly (distortions of the anomaly shape and intensity).
- (4) The variations in the shape of the electron density vertical profile.

If regularity in the observed anomalous variations is revealed, we will try to develop the mask of an ionospheric precursor for this region.

### 3. EARTHQUAKE OF MAY 12, 2008, IN THE SICHUAN PROVINCE (CHINA)

The Wenchuan earthquake with a magnitude of  $M = 7.9$  (Richter scale) occurred on May 12, 2008, at the point with the coordinates  $31.015^\circ \text{ N}$ ,  $103.365^\circ \text{ E}$  (Fig. 1) in the zone of the Longmenshan fault, formed as a result of the collision between the Eurasian and Indo-European tectonic plates. The fault passes along the western margin of the Sichuan Basin, separating this basin from the Sino-Tibetan Mountains. This earthquake was characterized by an almost absolute absence of foreshocks and extremely high aftershock activity. The main shock factually stimulated the burst of seismic activity in this region, which lasted up to the end of May. Six hundred ninety seven earthquakes [<http://neic.usgs.gov/>] (including 126, 521, 48, and two events with magnitudes of  $3 \leq M < 4$ ,  $4 \leq M < 5$ ,  $5 \leq M < 6$ , and  $M = 6.0$  and  $6.1$ , respectively) occurred during this period. The time and magnitude distribution of the seismic energy is shown in Fig. 2, and the spatial distribution of seismic shocks is presented in Fig. 3. After the main shock of May 12, almost all shocks are concentrated along the Longmenshan fault, which indicates that these shocks are genetically interrelated and belong to the same process of tectonic reconstruction in this region of the Earth's crust.

### 4. EXPERIMENTAL DATA AND GEOPHYSICAL CONDITIONS

Since the data of the ground-based vertical sounding are unavailable in China, the available data from the IGS network GPS receivers were the main source of information about ionospheric variability in this region. We analyzed the data of *kunm*, *urum*, and *shao* receivers, the position of which is shown in Fig. 1.

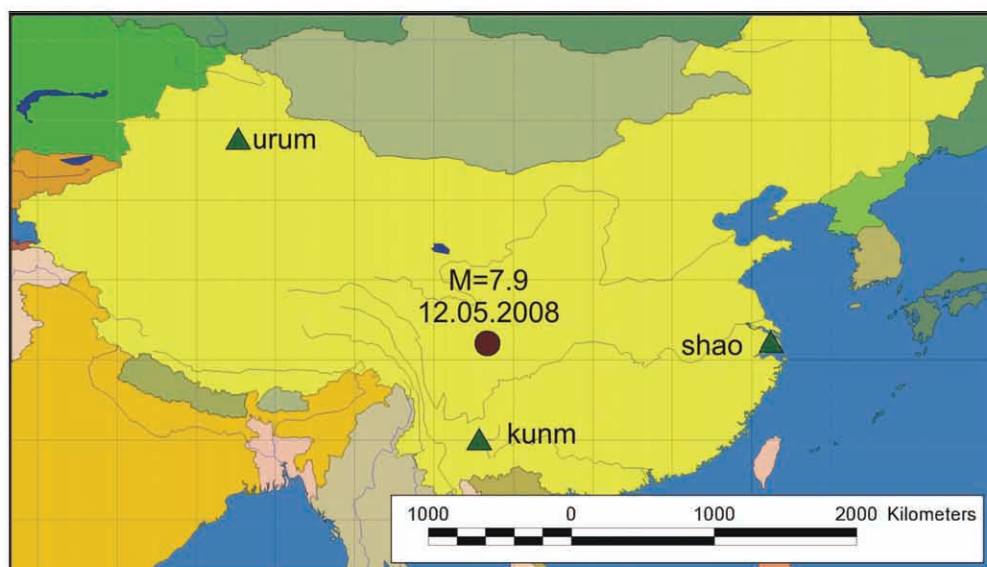


Fig. 1. The location of the epicenter of the Wenchuan earthquake, which occurred on May 12, 2008, and the GPS receivers.

*Kunm* station was located at the smallest distance to the epicenter and in the same longitudinal sector. The [Ciraolo and Spalla, 1997] method was used to calculate TEC in the vertical column. In addition, the IONEX (IONosphere Map EXchange) global ionospheric maps were used to analyze the global variations in the ionosphere. The index, calculated at the Polytechnical University of Catalonia (Barcelona) [Hernández-Pajares, 2003], was used as a data source. The dual-frequency sounding method [Bondur and Smirnov, 2005], which makes it possible to calculate the electron density vertical profiles at the subionospheric point on the line joining a satellite and a ground receiver, was used to reconstruct the electron density vertical profiles from the GPS data. In this case the position of the subionospheric point is selected in the earthquake preparation region.

The geomagnetic conditions during the earthquake preparation period were quiet. Figure 4, which presents the *Dst* index of geomagnetic activity, indicates that the value of this index was not larger than  $\pm 20$  nT beginning from April 29. An insignificant disturbance ( $Dst = -43$  nT) did not result in electron density variations outside the lower quartile. Geomagnetic activity was almost zero during  $\pm 5$  days after the main shock. During May 2008, the *Ap* and *Kp* indices were not more than 12 and 0–2, respectively. Dead geomagnetic calm made it possible to study ionospheric variations during seismic activity in the Sichuan province. This made it also possible to compare ionospheric variations over the seismic region with simultaneous variations far from this region.

## 5. TEC VARIATIONS

Figure 5a presents the TEC variations in the vertical column, calculated using the *kunm* data (a thick

solid line) from April 26 to May 26, 2008. A gray solid line presents a current monthly median, calculated for 30 days before a current day of TEC presentation. The lower and upper quartiles are shown by thin black and thick gray lines in Fig. 5b, respectively. Figure 5b indicates that the TEC current values are regularly observed outside the lower and upper quartiles in spite of quiet geomagnetic conditions. In this case we should note that the background of deviations is mainly negative before the earthquake, and intense positive deviations are observed immediately after the earthquake. We can note that negative deviations appeared every day at the same time (1400–1600 LT) during several days before the main shock of May 12, which is one of the morphological indications of ionospheric earthquake precursors according to Section 2. The relative TEC deviations are shown in Fig. 5c. The local time corresponds to the time when negative TEC deviations were registered before strong earthquakes on Taiwan [Liu et al., 2004].

Negative deviations were registered during three days more, and an intense positive deviation was observed May 16. This process came to the end on May 20, when the main period of seismic activity terminated (see Fig. 2).

## 6. EQUATORIAL ANOMALY DYNAMICS

Taking into account the fact that the earthquake epicenter and *kunm* and *shao* stations are located on the outer slope of the equatorial anomaly northern crest, we should consider the anomaly dynamics during the earthquake preparation period. For this purpose, we studied the dynamics of the equatorial anomaly latitudinal section according to the IONEX data at a latitude of  $105^\circ$  E almost coinciding with the epicenter longitude (Fig. 6). Taking into account the fact that

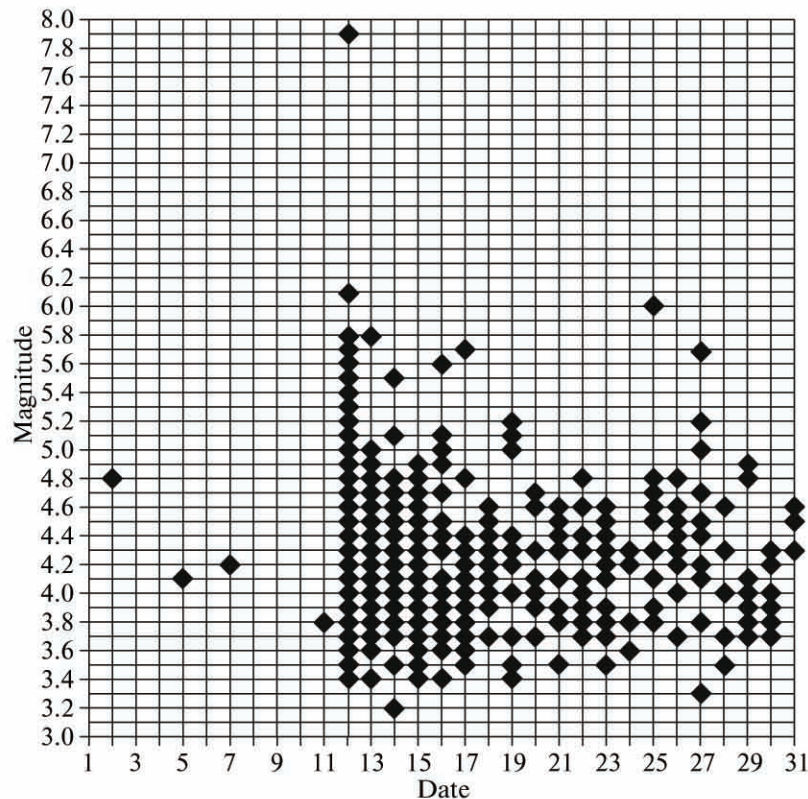


Fig. 2. The earthquakes with  $M > 3$ , which occurred in China on May 1–31, 2008.

the equatorial anomaly development maximum is observed in the afternoon hours, we constructed the latitudinal sections for 1400 LT. The following effects were registered: (a) the electron content in the equatorial anomaly was generally depressed; (b) the equatorial anomaly shape was distorted, and the southern crest was strongly depressed and completely disappeared; and (c) the equatorial anomaly crests moved toward the geomagnetic equator during the period of earthquake preparation and high seismic activity.

We consider these effects in more detail. Figure 6a, which presents all sections of the equatorial anomaly from April 26 to May 25, indicates that the electron density in the equatorial anomaly (the curve area) is minimal on the earthquake day of May 12 (colored black). In this case the anomaly southern crest is almost absent.

We now consider the anomaly shape (Fig. 6b). On April 26 and 27, the anomaly shape corresponds to the season [Mendillo et al., 2005] (the southern crest is higher than the northern one since the period of the vernal equinox has been passed); however, the southern crest is sharply depressed on April 29. In this case the anomaly shape on April 29 is the same as on May 12, but the electron density is higher. The anomaly restores its seasonal shape only by the end of May (on May 24). We should bear in mind that seismic activity remained high during a month after the main shock, as

a result of which the state of the ionosphere was disturbed and the electron density was decreased during a long period.

A low latitudinal resolution of the IONEX index ( $2.5^\circ$ ) did not make it possible to study in detail the motion of the equatorial anomaly crests depending on latitude; nevertheless, Fig. 6c evidently demonstrates that these crests moved toward the geomagnetic equator as we approach the earthquake instant and during the entire period of seismic activity. A thin broken line in Fig. 6c shows the positions of the northern and southern crests of the equatorial anomaly, and a thick line demonstrates the current average positions of the crests during five days. A horizontal straight line marks the geomagnetic equator latitude at a longitude of  $105^\circ$  E ( $8.2^\circ$  N). The equatorial anomaly crests started drawing together from April 21. April 29, when the equatorial anomaly southern crest is not identified, is one of the most anomalous days. The crests continued approaching the geomagnetic equator during the entire seismic period, and this approach was maximal on May 18 (a week before the second-magnitude ( $M=6$ ) shock in the series that took place on May 25). Figure 6 indicates that the latitudinal displacements of the northern and southern crests of the equatorial anomaly can exceed  $5^\circ$  on some days and even during several days.

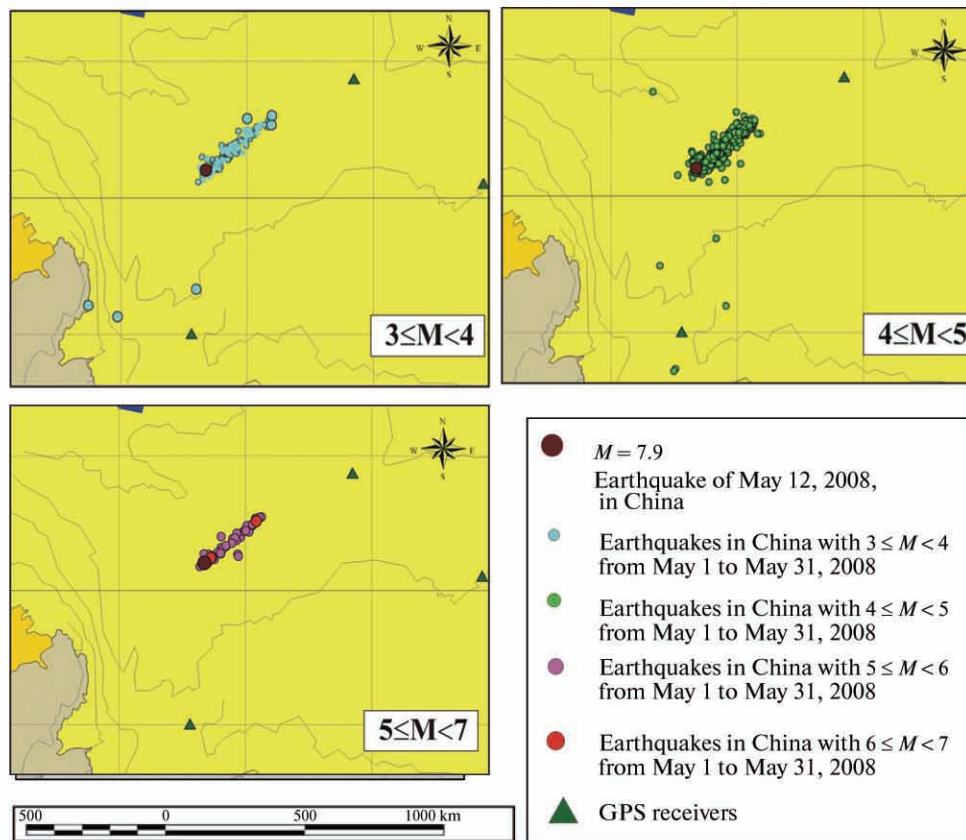


Fig. 3. The location of the epicenters of the earthquakes with  $M > 3$ , which occurred in China on May 1–31, 2008.

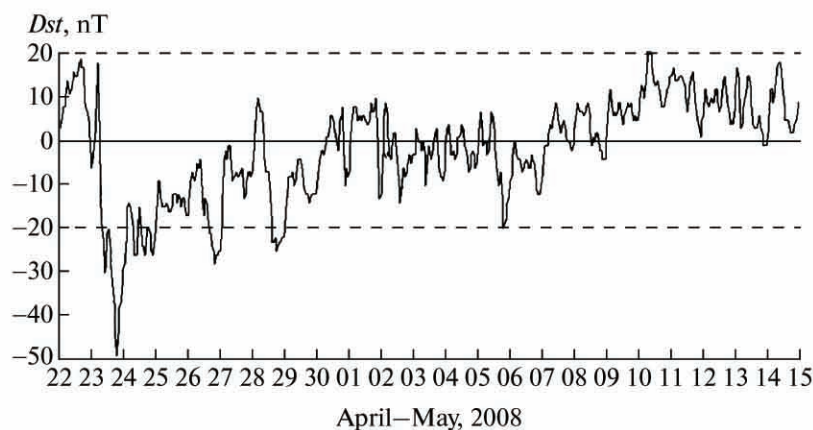
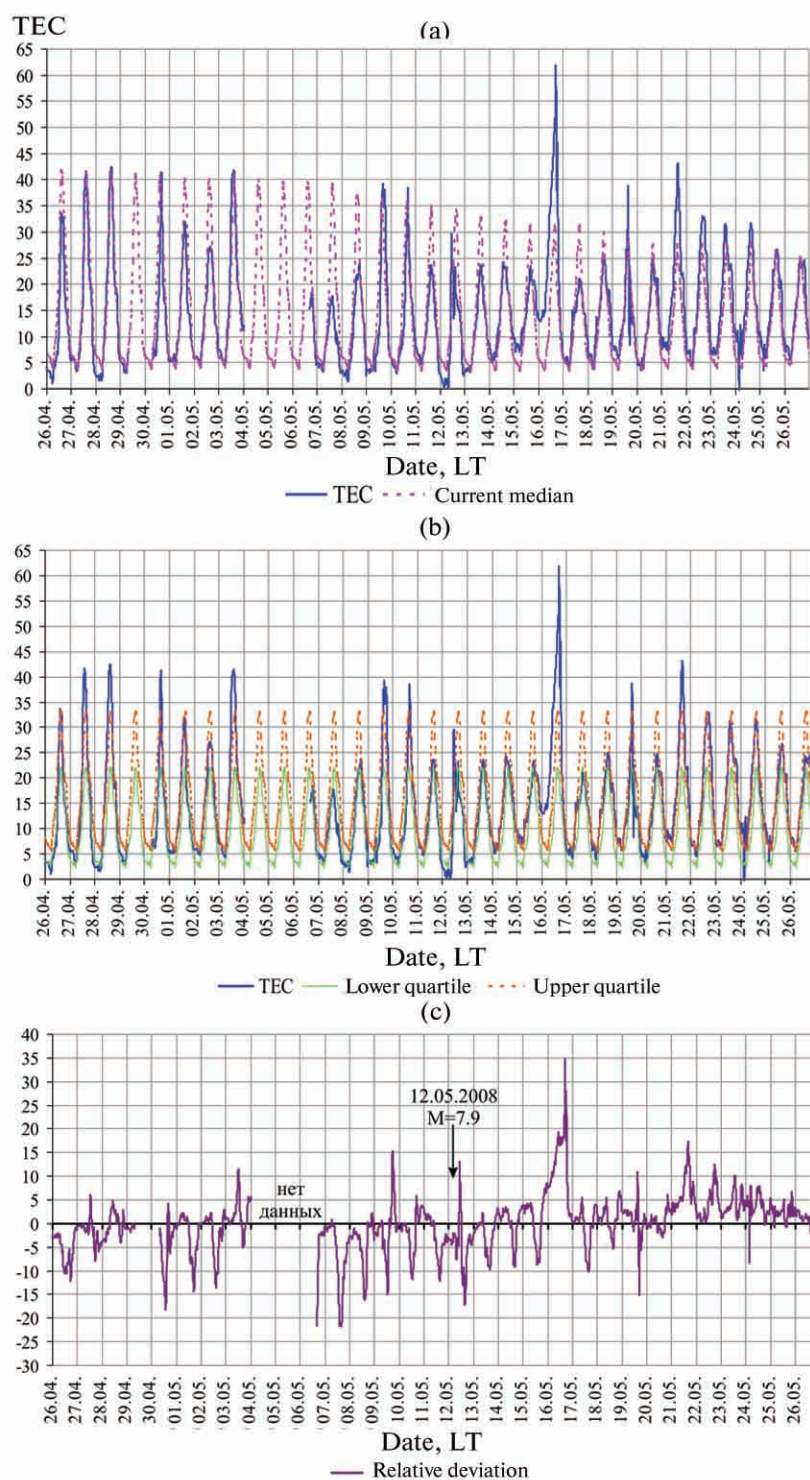


Fig. 4. The  $Dst$  equatorial geomagnetic index from April 22 to May 15, 2008.

Note that the equatorial anomaly shape is distorted (the seasonal asymmetry) only in the longitudinal sector near the epicenter. The equatorial anomaly southern crest was higher than the northern crest already at a longitude of  $80^\circ$  E for the entire period from the end of April to May 12.

## 7. DYNAMICS OF ELECTRON DENSITY VERTICAL PROFILES

Bondur and Smirnov [2005] proposed the method for reconstructing electron density vertical profiles using data of navigation systems. For the GPS 31 satellite, which was over the horizon during the Wen-



**Fig. 5.** The time variations in (a) TEC and the current median, (b) TEC (the lower and upper quartiles), and (c) relative deviations from April 26, 2008, to May 26, 2008, according to *kunm* GPS receiver.

chuan earthquake preparation, the electron density vertical profiles were calculated for 1600 LT from April 27 to May 14. In this case the position of the subionospheric point was near the epicenter and *kunm* station during several hours (see Fig. 7). The electron density

dynamics at the  $F_2$  layer maximum confirms the result achieved based on the IONEX index data: the electron density decreased as we approach the seismic shock instant. The variations in the  $NmF_2$  electron density from April 27 to May 12 are  $\sim 500\%$ . The electron den-

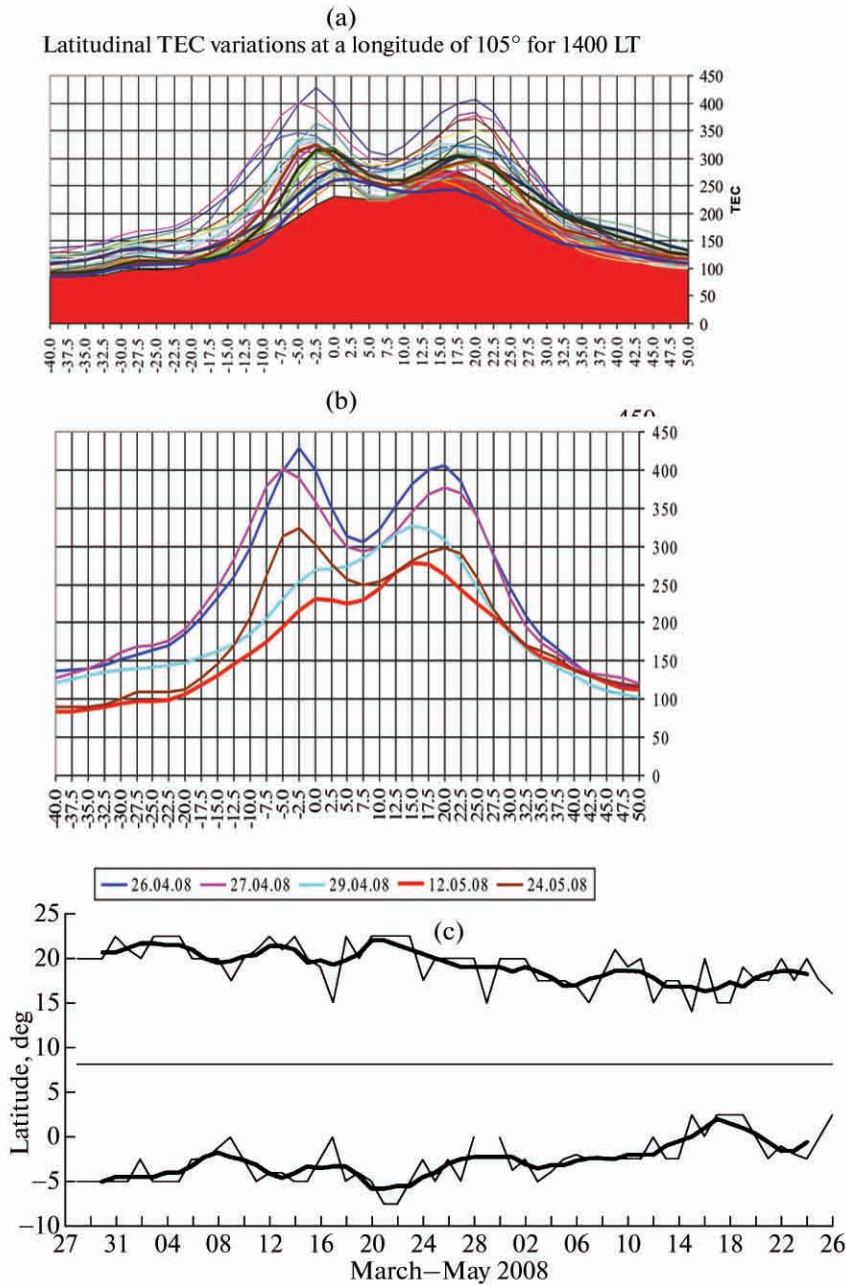


**Fig. 6.** (a) the TEC latitudinal sections at a longitude of 105° E in the equatorial anomaly region from April 26 to May 25; (b) the variations in the equatorial anomaly shape at a longitude of 105° E before and after the Wenchuan earthquake; and (c) the latitude of the equatorial anomaly crests and a longitude of 105° E during the Wenchuan earthquake.

sity was minimal ( $4.56 \times 10^5 \text{ cm}^{-3}$ ) on May 7, five days before the main seismic shock, which is a factor of 5 as low as the density value on April 27 ( $2.27 \times 10^6 \text{ cm}^{-3}$ ), see Fig. 8a.

For the calculated profiles, we studied the behavior of the scale height. As a preliminary estimate we used a difference between the height, where the density is lower than the density at the  $h_{[HmF2/e]}$  maximum, and  $HmF2$ :

$$H = h_{[HmF2/e]} - HmF2.$$

The variations in the  $H$  values indicates that the scale height increases by 15 km as we approach the earthquake instant, which confirms the dependence described in [Pulinets et al., 2007]. The scale height started decreasing after the earthquake (Fig. 8b).

## 8. LOCALIZATION OF IONOSPHERIC ANOMALIES

In the absence of the satellite methods for vertical sounding the ionosphere, which would make it possi-

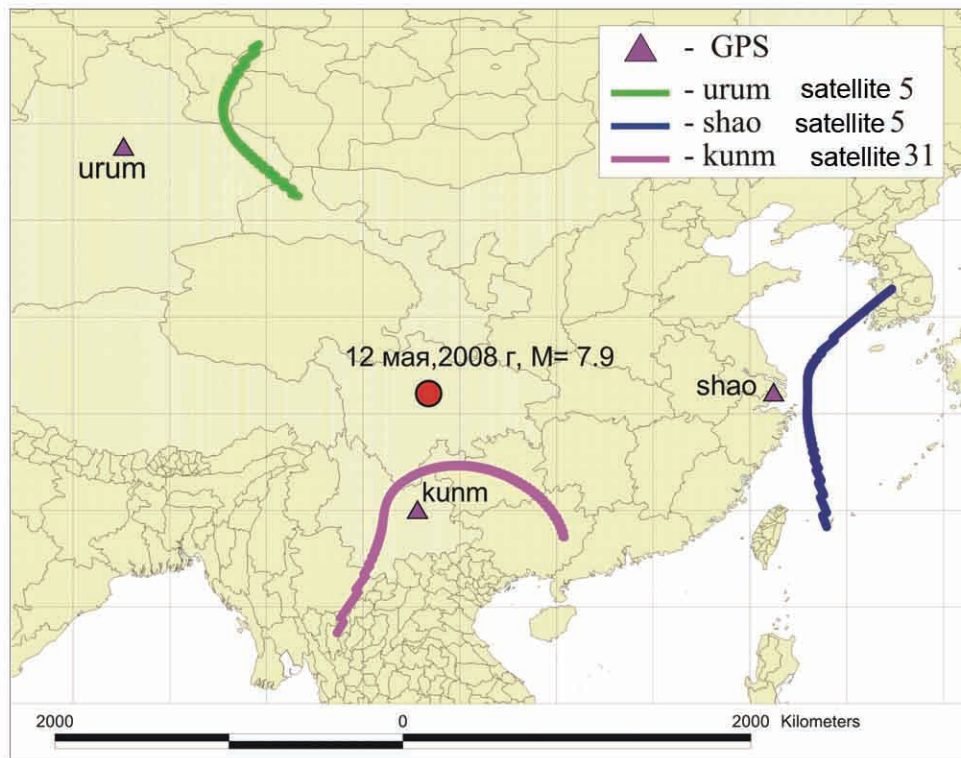


Fig. 7. The map of the subionospheric point trajectories for the GPS 5 and 31 satellites.

ble to globally map the ionosphere and determine the position of ionospheric anomalies related to seismic activity [Pulinets and Legen'ka, 2003], the global TEC maps, created using the IONEX index [Hernández-Pajares, 2003], are the most adequate method. Taking into account the fact that the maximal variability of the low-latitude ionosphere is related to the equatorial anomaly dynamics, we analyzed the maps for 0800 UT, which corresponds to 1600 LT (Fig. 9) for the longitude of the earthquake epicenter and the maximum in the development of the equatorial anomaly. To reveal the variability of the ionosphere, we constructed the maps of TEC deviation from the average monthly values. The data of the point measurements at the ground stations made it possible to determine the most anomalous days: April 29, May 9, etc. The global maps generally confirm the registered dynamics, but several specific features, which cannot be determined based on point measurements, are revealed in this case:

(1) The variability is maximal south of the epicenter and at crests of the equatorial anomaly rather than exactly over the epicenter.

(2) The longitudinal effect is observed, when deviations of different signs are registered on the left and right of the epicenter (on May 3 and 9).

(3) A global longitudinal ionospheric inhomogeneity with an extremely large amplitude (about  $\pm 20$  TEC) was formed on the day of earthquake 2 h

after the shock. In this case negative and positive deviations were mainly observed west and east of the epicenter, respectively. A global inhomogeneity existed during three days after the shock and then disappeared.

(4) The deviation was mostly observed at both crests of the equatorial anomaly rather than at the northern crest, which was the closest formation to the epicenter.

The figures indicate that ionospheric anomalies are concentrated around the impending earthquake epicenter in longitude, their latitudinal extension reaches  $40^\circ$ , and the longitudinal position varies from  $60^\circ$  to  $120^\circ$  on different days. Disturbances in the low-latitude ionosphere are global during three days after the earthquake. The morphology of the observed phenomena indicates that the zonal electric field, resulting in the generation of the equatorward electrojet and modification of the equatorial anomaly, is the main disturbing factor [Klimenko et al., 2006].

## 9. CREATION OF EARTHQUAKE MASK

The statistical studies of ionospheric effects on Taiwan [Pulinets et al., 2002; Liu et al., 2006] made it possible to detect that ionospheric variations observed by a ground station (ionosonde or GPS receiver) are similar for different earthquakes if the epicenters of these earthquakes are in the same seismic region. This

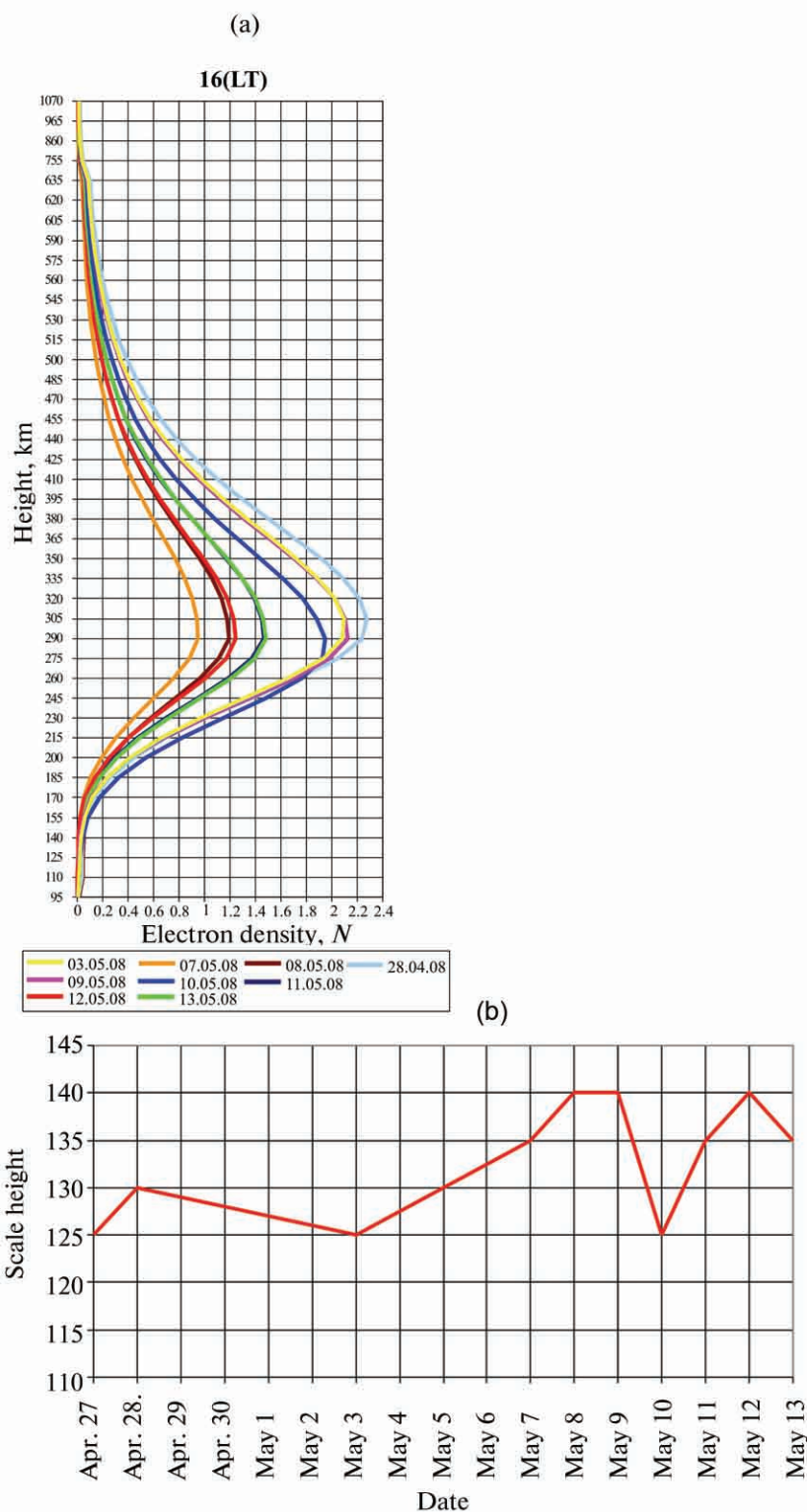


**Fig. 8.** (a) The electron density vertical profiles, reconstructed using the TEC data for 1600 LT from April 27 to May 13, 2008; (b) the variations in the scale height of the electron density vertical profiles presented in Fig. 8a.

made it possible to put forward the concept of the so-called ionospheric precursor mask: the three-dimensional representation of anomalous variations in coor-

dinates days to earthquake—local time—deviation amplitude. Since the mask construction method was described in detail by Pulinets et al. [2002], we will

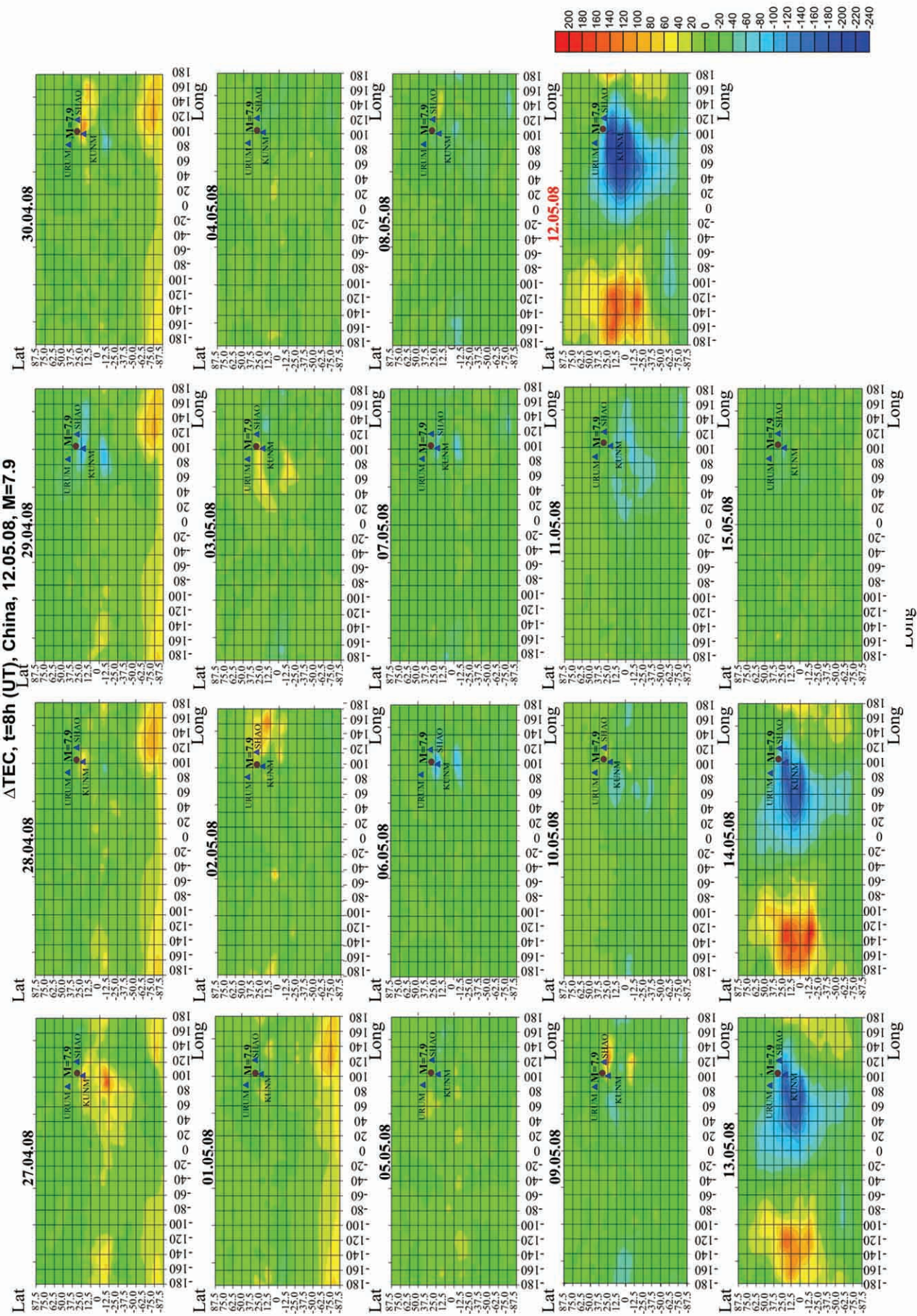
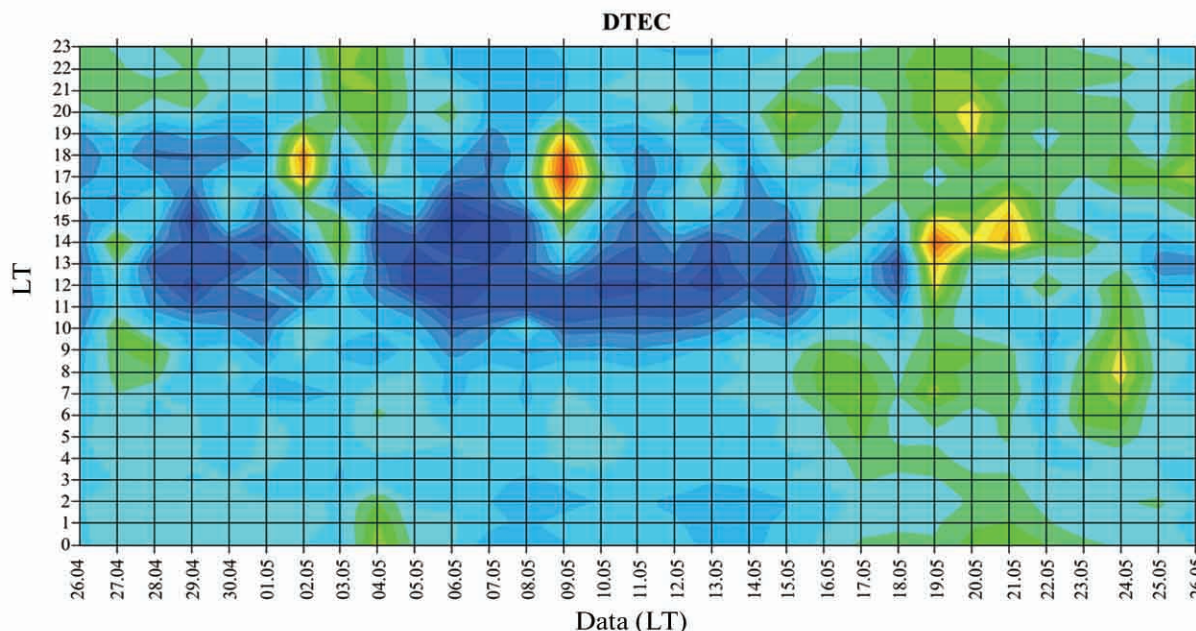


Fig. 9. The variations in the global distribution of the TEC deviation from the average monthly value according to the IONEX data for the period from April 27 to May 15, 2008.



**Fig. 10.** The ionospheric precursor mask from April 26 to May 26, 2008, during the preparation of the earthquake ( $M = 7.9$ ) that occurred in China on May 12, 2008 (the *shao* GPS station data).

omit this procedure and immediately analyze the obtained data. Considering that there are gaps in the *kunm* data, we used the data of *shao* station (see Fig. 10) in order to construct masks of the Wenchuan earthquake. As in the Taiwan case [Liu et al., 2000], negative variations in the postnoon hours are the main observed effect. These variations are observed from April 29 to May 15. The longest interval of daily negative variations (from 1000 to 1600 LT) was observed on May 6 (six days before the earthquake). The obtained mask is almost identical to the mask for Taiwan; the only difference consists in that the present work considered the longer interval of observations before and after the earthquake. This confirms the conclusion that the ionospheric precursors are similar and depend on the local time.

## 10. DISCUSSION OF RESULTS

An analysis of the ionospheric parameters, obtained using the GPS system, indicated that all morphological indications of ionospheric earthquake precursors described in the literature are present in the registered variations during the preparation of the Wenchuan earthquake. A very low level of solar and geomagnetic activity makes it possible to state that the observed global variations were mainly caused by seismic activity. The local time of the maximal variations corresponds to the time when the equatorial anomaly was most developed. The global maps and equatorial anomaly latitudinal profiles make it possible to state that the observed variations were caused by additional electric fields, which disturb the normal daily varia-

tions in the development of the equatorial anomaly. The seasonal asymmetry of the equatorial anomaly is usually related to the thermospheric wind directed from the summer hemisphere to the winter one [Mendillo et al., 2001]; however, in this case a disturbance of the shape of the equatorial anomaly crests can hardly be explained by thermospheric winds. Most probably, we should also consider the possible appearance of anomalous zonal and meridional electric fields. At the very least, we should consider the possible meridional gradient of the zonal electric field. When electric field effects are modeled, a similar approach makes it possible to explain anomalies observed before earthquakes in the low-latitude ionosphere [Namgaladze et al., 2009]. The mechanism by which an anomalous electric field is generated before earthquakes is described in [Pulinets, 2009a]. Thus, we can consider that the observed effects have been explained in the scope of the proposed physical models.

In addition to the fact that the main indications of the ionospheric precursors of the Wenchuan earthquake are similar to the indications detected previously and described in the literature, we should refer to several new results and differences. Negative deviations begin to manifest themselves long before the statistically defined lead time (five days). They appear from April 29, i.e., two weeks before the main shock. We detected the longitudinal–latitudinal asymmetry of the earthquake preparation region in the ionosphere. The latitude of the preparation region corresponds to the data obtained in [Dobrovolskii, 1991]; at the same time, the zonal extension of this region much exceeds these data, which is apparently related

to the mechanisms by which the equatorward electrojet is formed. A global disturbance of the low-latitude ionosphere during three days after the earthquake is absolutely unexpected. Such a phenomenon was observed for the first time and should be interpreted.

### ACKNOWLEDGMENTS

This work used the data of the research scientific works, performed in the scope of the Federal Special Program "Scientific and Pedagogical Personnel in Innovation Russia" for 2009–2013.

### REFERENCES

- E. L. Afraimovich and E. I. Astafyeva, "TEC Anomalies - Local TEC Changes Prior to Earthquakes or TEC Response to Solar and Geomagnetic Activity Changes?," *Earth Planet. Space* **60**, 961–966 (2008).
- V. G. Bondur and V. M. Smirnov, "A Method of Earthquake Forecast Based on the Lineament Analysis of Satellite Images," *Dokl. Akad. Nauk* **402** (5), 675–679 (2005) [*Dokl. Earth Sci.* **402** (4), 561–568 (2005)].
- J. Bošková, J. Šmilauer, F. Jiříček, and P. Tříška, "Is the Ion Composition of Outer Ionosphere Related to Seismic Activity," *J. Atmos. Terr. Phys.* **55**, 1689–1695 (1993).
- Y. J. Chuo, Y. I. Chen, J. Y. Liu, and S. A. Pulinet, "Ionospheric *foF2* Variations Prior to Strong Earthquakes in Taiwan Area," *Adv. Space Res.* **27**, 1305–1310 (2001).
- L. Ciraolo and P. Spalla, "Comparison of Ionospheric Total Electron Content from the Navy Navigation Satellite System and the GPS," *Radio Sci.* **32**, 1071–1080 (1997).
- I. P. Dobrovolskii, *Theory of Tectonic Earthquake Preparation* (Inst. Fiz. Zemli Akad. Nauk SSSR., Moscow, 1991) [in Russian].
- M. Hernández-Pajares, [http://maite152.upc.es/~ionex3/doc/IPS\\_IONO\\_report\\_April2003\\_7.pdf](http://maite152.upc.es/~ionex3/doc/IPS_IONO_report_April2003_7.pdf).
- M. V. Klimenko, V. V. Klimenko, and V. V. Bruykanov, "Numerical Simulation of the Electric Field and Zonal Current in the Earth's Ionosphere: The Dynamo Field and Equatorial Electrojet," *Geomagn. Aeron.* **46** (4), 457–466 (2006) [*Geomagn. Aeron.* **46**, 457 (2006)].
- J. Y. Liu, Y. I. Chen, S. A. Pulinet, et al., "Seismo-Ionospheric Signatures Prior to  $M \geq 6$  Taiwan Earthquakes," *Geophys. Res. Lett.* **27**, 3113–3116 (2000).
- J. Y. Liu, Y. I. Chen, Y. J. Chuo, and C. S. Chen, "A Statistical Investigation of Preearthquake Ionospheric Anomaly," *J. Geophys. Res.* **111**, A05304 (2006).
- J. Y. Liu, Y. J. Chuo, S. J. Shan, et al., "Pre-Earthquake Ionospheric Anomalies Registered by Continuous GPS TEC Measurements," *Ann. Geophys.* **22**, 1585–1593 (2004).
- M. Mendillo, C.-L. Huang, X. Pi, H. Rishbeth, and R. Meier, "The Global Ionospheric Asymmetry in Total Electron Content," *J. Atmos. Solar-Terr. Phys.* **67**, 1377–1387 (2005).
- A. A. Namgaladze, M. V. Klimenko, V. V. Klimenko, and I. E. Zakharenkova, "Physical Mechanism and Mathematical Modeling of Earthquake Ionospheric Precursors Registered in Total Electron Content," *Geomagn. Aeron.* **49** (2), 267–277 (2009) [*Geomagn. Aeron.* **49**, 252–262 (2009)].
- S. A. Pulinet and A. D. Legen'ka, "Dynamics of the Near-Equatorial Ionosphere Prior to Strong Earthquakes," *Geomagn. Aeron.* **42** (2) (2002) [*Geomagn. Aeron.* **42**, 227–232 (2002)].
- S. A. Pulinet and A. D. Legen'ka, "Spatial-Time Characteristics of Large-Scale Electron Density Inhomogeneities, Observed in the Ionospheric *F* Region before Strong Earthquakes," *Kosm. Issled.* **41** (3), 221–229 (2003).
- S. A. Pulinet and K. A. Boyarchuk, *Ionospheric Precursors of Earthquakes* (Springer, Berlin, 2004).
- S. A. Pulinet, "Lithosphere–Atmosphere–Ionosphere Coupling (LAIC) Model," in *Electromagnetic Phenomena Associated with Earthquakes*, Research Signpost, Japan, Chapter 9, 235–253 (2009a).
- S. A. Pulinet, "Physical Mechanism of the Vertical Electric Field Generation over Active Tectonic Faults," *Adv. Space Res.* **44**, 767–773 (2009b).
- S. A. Pulinet, "Seismic Activity as a Source of the Ionospheric Variability," *Adv. Space Res.* **22**, 903–906 (1998).
- S. A. Pulinet, A. D. Legen'ka, T. V. Gaivoronskaya, and V. K. Depuev, "Main Phenomenological Features of Ionospheric Precursors of Strong Earthquakes," *J. Atmos.–Solar Terr. Phys.* **65**, 1337–1347 (2003).
- S. A. Pulinet, A. D. Legen'ka, and T. I. Zelenova, "Local-Time Dependence of Seismo-Ionospheric Variations at the *F*-Layer Maximum," *Geomagn. Aeron.* **38** (3), 188–193 (1998b) [*Geomagn. Aeron.* **38**, 400–402 (1998b)].
- S. A. Pulinet, K. A. Boyarchuk, A. M. Lomonosov, et al., "Ionospheric Precursors to Earthquakes: A Preliminary Analysis of the *foF2* Critical Frequencies at Chung-Li Ground-Based Station for Vertical Sounding of the Ionosphere (Taiwan)," *Geomagn. Aeron.* **42** (4), (2002) [*Geomagn. Aeron.* **42**, 508–513 (2002)].
- S. A. Pulinet, P. Biagi, V. Tramutoli, A. D. Legen'ka, and V. Kh. Depuev, "Irpinia Earthquake 23 November 1980 - Lesson from Nature Revealed by Joint Data Analysis," *Annals of Geophysics* **50**, 61–78 (2007).
- S. A. Pulinet, V. V. Khagai, K. A. Boyarchuk, and A. M. Lomonosov, "Atmospheric Electric Field as a Source of Ionospheric Variability," *Usp. Fiz. Nauk* **41** (5), 582–589 (1998a) [*Physics-Uspekhi* **41**, 515–522 (1998a)].
- I. E. Zakharenkova, A. Krankowski, and I. I. Shagimuratov, "Modification of the Low-Latitude Ionosphere before the 26 December 2004 Indonesian Earthquake," *Nat. Hazard Earth Syst. Sci.* **6**, 817–823 (2006).